Polish J. Chem., **78**, 1431–1447 (2004)

Electrochemical Formation of Two-component Films from 2′-Ferrocenylpyrrolidino[3′,4′;1,2][C_{60}]fullerene and Transition Metal Complexes*

by M.E. Płońska[1], A. Makar[1], K. Winkler[1] and A.L. Balch[2]****

[1]*Institute of Chemistry, University of Białystok, Hurtowa 1, 15-399 Białystok, Poland*
[2]*Department of Chemistry, University of California, Davis, CA 95616, USA*

(Received February 27th, 2004; revised manuscript May 7th, 2004)

Redox active films have been generated electrochemically by reduction of the chemically modified fullerene, 2′-ferrocenyl-pyrrolidino[3′,4′;1,2][C_{60}]fullerene – FcC_{60}, and [Pt(μ-Cl)Cl(C_2H_4)]$_2$ or Ir(CO)$_2$Cl(*p*-toluidine). The film is believed to consist of polymeric network formed *via* covalent bonds between the metal atoms and the fullerene moieties. Ferrocene is covalently linked to the polymeric chains through the pyrrolidine rings. The FcC_{60}/Pt film is electrochemically active in both positive and negative potential ranges. At positive potentials, oxidation of the appended ferrocene is observed. In the negative potential range, electron transfer processes involving the fullerene take place. FcC_{60}/Pt films exhibit higher permeability to anions than to cations. Only an outermost layer of this film is reduced. During the oxidation of the film significant structural changes occur. Film formation is also accompanied by platinum deposition. The present of a metallic phase in the film influences its morphology, structure and electrochemical properties. An FcC_{60}/Ir film has been formed during reduction of solutions containing both FcC_{60} and Ir(CO)$_2$Cl(*p*-toluidine). The yield of this film is low with only very thin layer deposited on the electrode surface. No electrochemical activity of the electrode modified with FcC_{60}/Ir was detected in acetonitrile containing only supporting electrolyte.

Key words:electropolymerization, ferrocene, fullerene, platinum, iridium, conducting polymer modified electrode

The preparation and characterization of π-conjugated polymers have received considerable attention in the field of materials science due to their exceptional redox properties. A number of these polymers can be synthesized under electrochemical conditions. Thus, much has been published on the electrochemical preparation and properties of conducting polymers such as polypyrrole [1–3], polyaniline [4–6] or polythiophene [7–9]. These materials have a wide range of promising applications in the fields of energy storage, electrocatalysis, organic electrochemistry, bioelectrochemistry, photochemistry, microsystem technologies, electronic devices, and corrosion protection [10–13].

Considerable effort has gone into the synthesis and study of new monomers for electropolymerization. From this point of view, fullerene molecules are very attractive. Up to six, reversible, one-electron steps can be observed for reduction of C_{60} in

* Dedicated to Prof. Dr. Z. Galus on the occasion of his 70th birthday.
** Corresponding authors

solution [14]. These electrode processes result from the sequential filling of the triply degenerated LUMO of C_{60}. Additionally, a one-electron oxidation is also observed for C_{60} at a relatively high potential [15].

Recently, new electro-synthetic procedures for the preparation of fullerene-based, redox-active films have been developed [16–25]. Two-component films prepared from fullerenes and transition metal complexes are particularly interesting because of their redox activity and their stability over a wide potential range [21,22,25–29]. These films can be readily prepared by electrochemical reduction of solutions that contain both C_{60} (or C_{70}) and selected transition metal complexes. The films are believed to be built from fullerene cages covalently bound to transition metal atoms or their complexes.

Polymers containing fullerene moieties that can undergo both *p*- and *n*-doping have also been prepared electrochemically. These "double cable" materials can be divided into two classes. In the first class, the fullerenes can be incorporated into an electron-donating conjugated polymer backbone [16,17,23]. In the second class, the electron-donating groups can be bonded to the polymeric chain which contains the fullerenes. Recently we have electropolymerized 2′-ferrocenylpyrrolidino-[3′,4′;1,2][C_{60}]fullerene in the presence of palladium acetate [25]. In this system, electron-accepting fullerene moieties are bounded *via* palladium atoms to form the polymer backbone, and the electron-donating ferrocene groups are covalently linked to it. This film exhibits electrochemical activity at both negative and positive potentials. The reduction of the film at negative potentials is related to the presence of C_{60} cages in the polymeric backbone. In the positive potential range, the oxidation of ferrocene groups takes place.

In this paper we examine the formation of new polymeric films prepared by reduction of 2′-ferrocenylpyrrolidino-[3′,4′;1,2][C_{60}]fullerene, **1**, and several other transition metal complexes. Previous work with C_{60} itself revealed that the complexes $[Pt(\mu\text{-}Cl)Cl(C_2H_4)]_2$, $Ir(CO)_2Cl$(*p*-toluidine), and $Rh_2(CF_3CO_2)_4$ were reasonable precursors for the deposition of redox active films [21,22,26–29]. Consequently we have examined these complexes as precursors for film formation with 2′-ferrocenylpyrrolidino-[3′,4′;1,2][C_{60}]fullerene. The electrochemical properties of new films have also been studied.

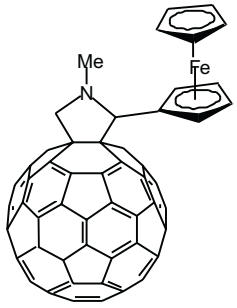

1

EXPERIMENTAL

Materials. 2′-Ferrocenylpyrrolidino[3′,4′;1,2][C_{60}]fullerene, FcC_{60}, was synthesized according to a method described in the literature [30,31]. Ferrocene carboxylaldehyde (Aldrich), di-μ-chloro-dichlorobis(ethylene)diplatinum(II) [Pt(μ-Cl)Cl(C_2H_4)]$_2$ (Strem Chemicals, MA), $Rh_2(CF_3CO_2)_4$ (Alfa) and C_{60} (Southern Chemical Group) were used as received. Ir(CO)$_2$Cl(*p*-toluidine) was prepared according to a procedure described in the literature [32]. The supporting electrolytes – tetra(*n*-butyl)ammonium perchlorate (Sigma Chemical Co.), tetra(*n*-butyl)ammonium hexafluorophosphate (Sigma Chemical Co), tetra(*n*-butyl)ammonium tetrafluoroborate (Sigma Chemical Co.), tetra(*n*-butyl)ammonium tetraphenylborate (Sigma Chemical Co.), tetra(*n*-hexyl)ammonium perchlorate (Fluka), and tetra(ethyl)ammonium perchlorate (Fluka) – were dried under vacuum for 24 hours prior to use. Acetonitrile (99.9%, Aldrich Chemical Co.) was used as received. Toluene (Aldrich Chemical Co.) was purified by distillation over sodium under a dinitrogen atmosphere.

Instrumentation. Voltammetric experiments were performed on a potentiostat/galvanostat Model 283 (EG&G Instruments) with a three-electrode cell. A gold disk with a diameter of 1.5 mm (Bioanalytical Systems, Inc.) was used as the working electrode. Prior to the experiment, the electrode was polished with fine carborundum paper and then with a 0.5 μm alumina slurry. Subsequently, the electrode was sonicated in water to remove traces of alumina from the gold surface, washed with water, and dried. A silver wire immersed in 0.010 M silver perchlorate and 0.09 M tetra(*n*-butyl)ammonium perchlorate in acetonitrile that was separated from the working electrode by a ceramic tip (Bioanalytical Systems Inc.) served as the reference electrode. The counter electrode was a platinum tab with an area of about 0.5 cm^2.

Scanning electron micrograph images were obtained with the use of a LEO 435 vp microscope. The accelerating voltage of the electron beam was 15 kV.

Simultaneous voltammetric and piezoelectric microgravimetry experiments were carried out with a home built potentiostat and electrochemical quartz crystal microbalance, EQCM 5510, of the Institute of Physical Chemistry (Warsaw, Poland). The 14 mm diameter AT-cut, plano-convex quartz crystals with 5 MHz resonant frequencies were obtained from Omig (Warsaw, Poland). A 100 nm gold film, which was vacuum deposited onto the quartz crystal, served as the working electrode. The projected area of this gold electrode, which included a 5 mm diameter circular center spot and two contacting radial strips, was 0.24 cm^2. Unpolished quartz crystals were used for better adherence of the polymer film. The sensitivity of the mass measurement calculated from the Saurbrey equation was 17.7 ng Hz^{-1} cm^{-2}.

Film growth procedure and electroactivity studies. Ferrocenylpyrrolidino-[C_{60}]fullerene and transition metal complexes films were prepared by electroreduction of an acetonitrile/toluene (1:4, *v:v*) solution that contained both 2′-ferrocenyl-pyrrolidino[3′,4′;1,2][C_{60}]fullerene and the appropriate transition metal complex as well as the supporting electrolyte, 0.10 M tetra(*n*-butyl)ammonium perchlorate. Films were grown under cyclic voltammetry conditions at a potential sweep rate of 100 mV/s. The electrochemical properties of the film were studied in an acetonitrile solution containing only the supporting electrolyte. In this case, the electrode covered with the film was rinsed several times with an acetonitrile/toluene (1:4 *v:v*) solution and then placed in an acetonitrile solution containing 0.10 M of supporting electrolyte. The modified electrode was allowed to equilibrate for 10 min while degassing with argon in the new solution before electrochemical measurements were conducted.

RESULTS AND DISCUSSION

FcC_{60}/Pt film formation. The FcC_{60}/Pt polymer was synthesized by electrochemical reduction of an acetonitrile/toluene (1:4, *v:v*) mixture containing FcC_{60} and [Pt(μ-Cl)Cl(C_2H_4)]$_2$. Upon repeated scanning of the potential between –100 and –1300 mV an increase of current in the range of fullerene reduction was seen, as

shown in trace a of Fig. 1. During this time a new electroactive phase grew on the electrode surface. The electrode coated with this film was subsequently transferred to an acetonitrile solution containing only supporting electrolyte and cyclic voltammograms were recorded. The film retains the redox activity of FcC_{60} precursor as seen in trace b of Fig. 1. In the negative potential range, the currents R_2 and O_2 are related to electron transfer to the fullerene. Peaks O_1 and R_1, which are present at positive potentials, are attributed to ferrocene oxidation. An additional peak R_1' is observed at potentials close to –900 mV. This peak is present only if the potential of O_1 peak is reached in the positive-going cycle.

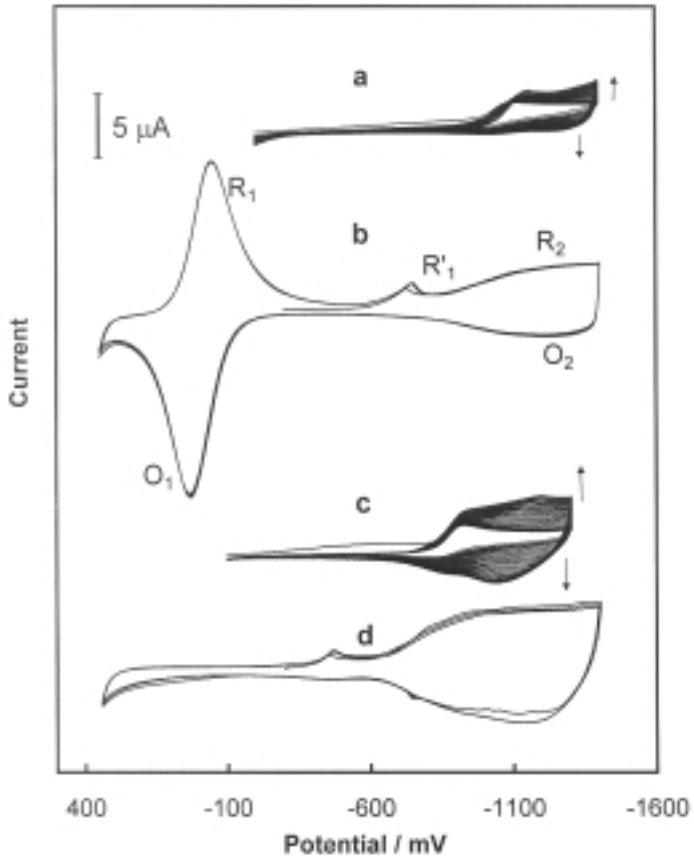

Figure 1. (a) Multicyclic voltammograms for 0.29 mM FcC_{60} and 0.37 mM $[Pt(\mu\text{-}Cl)Cl(C_2H_4)]_2$ in acetonitrile-toluene (1:4, *v:v*) containing 0.10 M tetra(*n*-butyl)ammonium perchlorate. (b) Multicyclic voltammograms for the FcC_{60}/Pt electropolymerized film in acetonitrile containing 0.10 M tetra(*n*-butyl)ammonium perchlorate. (c) Multicyclic voltammograms for 0.25 mM C_{60} and 0.42 mM $[Pt(\mu\text{-}Cl)Cl(C_2H_4)]_2$ in acetonitrile-toluene (1:4, *v:v*) containing 0.10 M tetra(*n*-butyl)ammonium perchlorate. (d) Multicyclic voltammograms for the C_{60}/Pt electropolymerized film in acetonitrile containing 0.10 M tetra(*n*-butyl)ammonium perchlorate. The sweep rate was 100 mV s^{-1}.

For comparison, multicyclicvoltammograms of the C_{60}/Pt film formation and cyclic voltammetric response of the polymer in acetonitrile containing only supporting electrolyte are shown in traces c and d, respectively of Fig. 1. For the same concentration of precursors the amount of solid phase deposited on the electrode surface is larger for C_{60}/Pt than for the FcC_{60}/Pt analog.

The process of FcC_{60}/Pt film formation was also investigated using an electrochemical quartz crystal microbalance. The frequency changes of the quartz crystal for the first four cycles of film formation are shown in Fig. 2. The frequency decreases in the negative-going cycle at potentials of the reduction of the platinum complex. There are almost no frequency changes in positive going cycle. It indicates that the film is not re-oxidized and remains doped with supporting electrolyte cations. The frequency changes are similar in each cycle. The potential at which the frequency

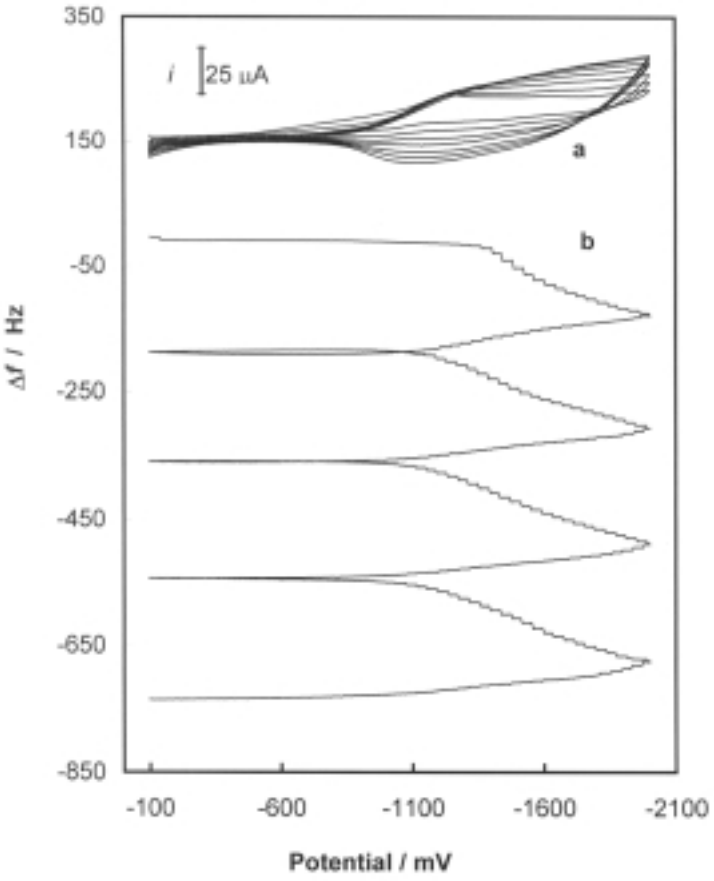

Figure 2. Multicyclic voltammograms (a) and curves of the frequency charge *vs*. potential (b) simultaneously recorded at the same Au/quartz electrode for 0.29 mM FcC_{60}/Pt and 0.40 mM $[Pt(\mu\text{-}Cl)Cl(C_2H_4)]_2$ in acetonitrile-toluene (1:4, *v:v*) containing 0.10 M tetra(*n*-butyl)ammonium perchlorate. The sweep rate was 100 mV s^{-1}.

decreases shifts toward less negative values with an increase of the scan number. The mass of material deposited on the electrode surface in each cycle is equal to about 3000 ng/cm^2. Assuming that the mass of monolayer doped with tetra(*n*-butyl)ammonium cations is equal to 130 ng/cm^2 [28], about 20 monolayers are deposited in each cycle under typical voltammetric conditions.

The morphology of the FcC_{60}/Pt film formed at the surface of a gold electrode is shown in Fig. 3. The film consists of the densely packed irregular grains about 0.5 μm thick. The surface of the film is relatively uniform.

Electrochemical properties of the FcC_{60}/Pt film. The effect of sweep rate on the voltammetric response of the electrode coated with a FcC_{60}/Pt film was investigated. The relevant data are shown in Fig. 4. The peak current for fullerene reduction increases linearly with the sweep rate. This observation indicates that the process is controlled by the rate of charge transport through the film. Similar behavior is observed for the peak for ferrocene oxidation (i_{pO1}) for low sweep rates. For sweep rates higher than about 200 mV/s, a departure from a linear i_{pO1}-v relation is observed (insert in Fig. 4). The shape of voltammetric peak for the ferrocene oxidation also changes with an increase of the sweep rate. That is, the peaks exhibit a characteristic, symmetric bell shape for a low sweep rate. In this case, no diffusion limitation occurs, and the overall electrode process depends on the rate of electron transfer throughout the film. For higher sweep rates, the voltammetric responses exhibit a characteristic tailing in the current at potentials following the peak. Such an asymmetric shape indicates that the diffusional transport of counter ions is the rate-limiting factor.

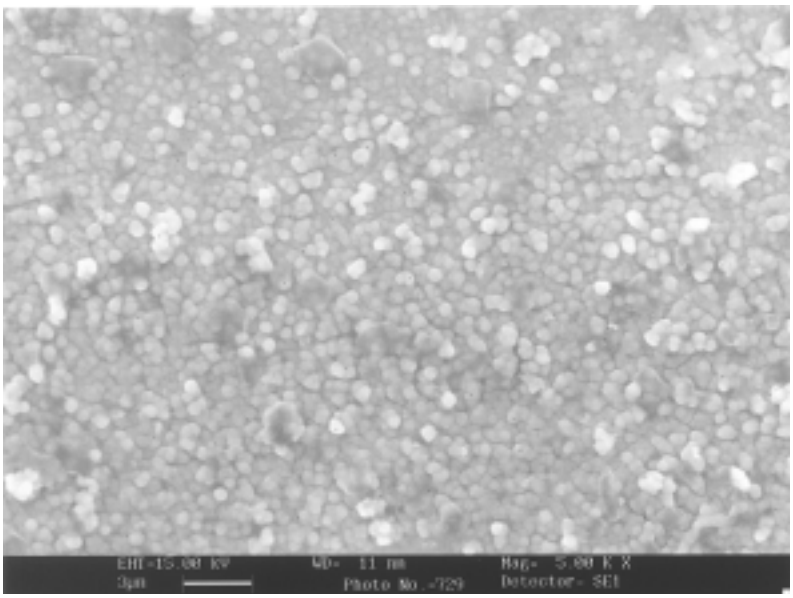

Figure 3. SEM image of the FcC_{60}/Pt film electropolymerized on the gold foil surface under cyclic voltammetry conditions (20 cycles) from 0.30 mM FcC_{60} and 0.37 mM $[Pt(\mu\text{-}Cl)Cl(C_2H_4)]_2$ in acetonitrile-toluene (1:4, *v:v*) containing 0.10 M tetra(*n*-butyl)ammonium perchlorate.

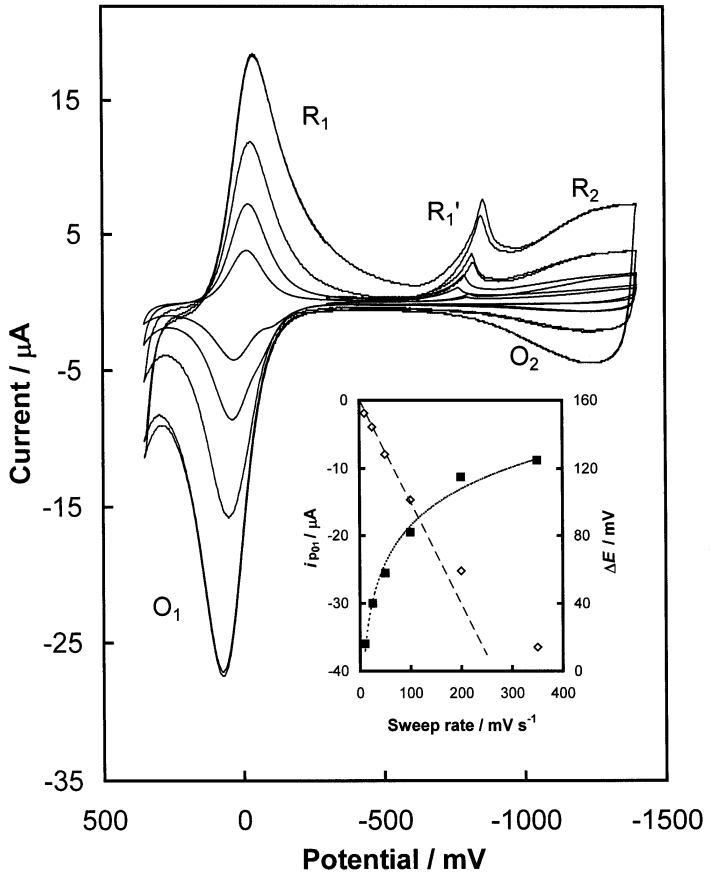

Figure 4. Cyclic voltammograms for the FcC_{60}/Pt film, prepared by electropolymerization in acetonitrile containing 0.10 M tetra(*n*-butyl)ammonium perchlorate for different sweep rates: 25 (innermost), 50, 100 and 200 mV/s (outermost) as well as the dependence of the O_1 peak current (open diamonds) and the difference between anodic, O_1, and cathodic, R_1, peak potentials (filled squares) on the sweep rate (inset graph). The FcC_{60}/Pt film was grown under cyclic voltammetry conditions in an acetonitrile-toluene (1:4, *v:v*) solution containing 0.29 mM FcC_{60}, 0.37 mM $[Pt(\mu\text{-}Cl)Cl(C_2H_4)]_2$ and 0.10 M tetra(*n*-butyl)ammonium perchlorate as supporting electrolyte.

The potential difference between the anodic O_1 and the cathodic R_1 peaks increases as the sweep rate increases. The peak difference changes from 25 mV to 140 mV for the sweep rate changes from 10 mV/s to 350 mV/s. The shift of the peak potentials with sweep rate is probably related to the changes of the resistance of the layer. The anodic peak potential linearly depends on the peak current. From the slope of this relation the resistance of layer equal to 1500 ohm was calculated. Since the resistance of solution was compensated the obtained value represents the resistance of the film. The approximate thickness of the film formed under those conditions is about 600 nm [28].

Assuming that the film forms a uniform layer the specific resistance of about 4500 Ω m was found.

The electrochemical properties of an electrode coated with the FcC_{60}/Pt film in acetonitrile containing variety of supporting electrolytes: tetra(ethyl)ammonium perchlorate, tetra(*n*-butyl)ammonium perchlorate, tetra(*n*-hexyl)ammonium perchlorate, tetra(*n*-butyl)ammonium tetrafluoroborate, tetra(*n*-butyl)ammonium hexafluorophospate and tetra(*n*-butyl)ammonium tetraphenylborate were investigated. Fig. 5 shows the results of these studies. Both the ferrocene involved oxidation and fullerene involved reduction processes are independent of the cation of the supporting electrolyte. However, the anions of supporting electrolyte do affect the process of ferrocene moiety oxidation. The separation between the anodic (E_{pO1}) and

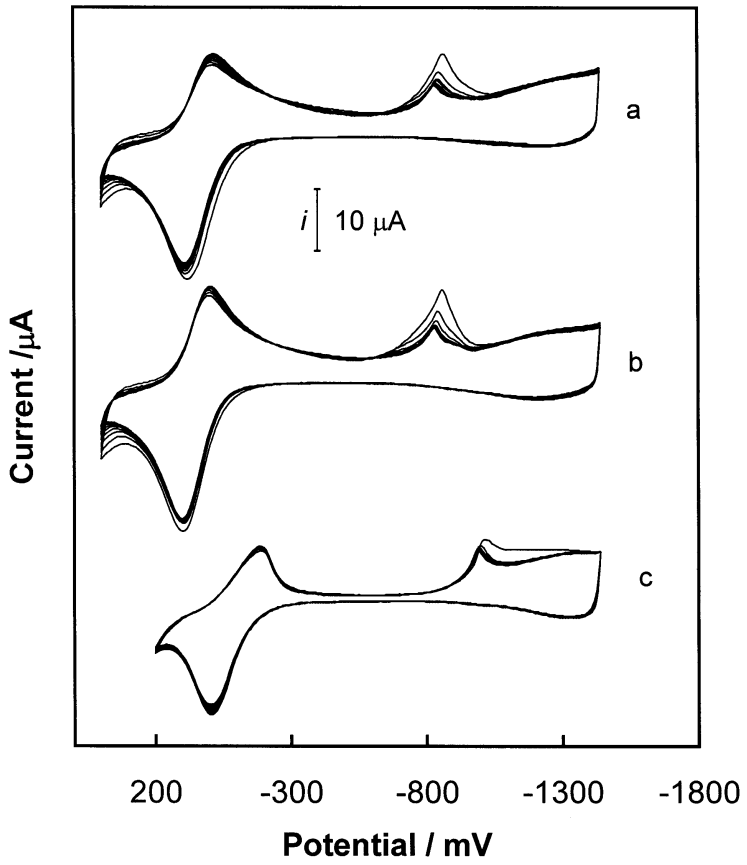

Figure 5. Cyclic voltammograms for the FcC_{60}/Pt films in acetonitrile containing (a) 0.10 M tetra(*n*-butyl)ammonium perchlorate, (b) 0.10 M tetra(*n*-hexyl)ammonium perchlorate, and (c) 0.10 M tetra(*n*-butyl)ammonium tetraphenylborate. The sweep rate was 100 mV/s. The FcC_{60}/Pt film was grown under cyclic voltammetry conditions in an acetonitrile-toluene (1:4, *v:v*) containing 0.29 mM FcC_{60}, 0.37 mM $[Pt(\mu\text{-}Cl)Cl(C_2H_4)]_2$ and 0.10 M tetra(*n*-butyl)ammonium perchlorate as supporting electrolyte.

cathodic (E_{pR1}) peak potentials increases with increases in the size of the anions of the supporting electrolyte.

The voltammetric response of the film depends on the composition of the solution used for film preparation. Fig. 6 shows the electrochemical properties of the films formed in acetonitrile/toluene (1:4, *v:v*) of a fixed concentration of FcC_{60} and different concentrations of $[Pt(\mu\text{-}Cl)Cl(C_2H_4)]_2$. An increase in the platinum complex concentration results in an increase in the reversibility of the ferrocene moiety oxidation. Eventually, peaks O_1 and R_1, obtained for the film formed in solution containing a large excess of $[Pt(\mu\text{-}Cl)Cl(C_2H_4)]_2$ become symmetrical (Fig. 6c).

The sweep rate effect on voltammograms of the FcC_{60}/Pt film deposited on the electrode surface in a solution containing 1.72 mM $[Pt(\mu\text{-}Cl)Cl(C_2H_4)]_2$ and 0.29 mM

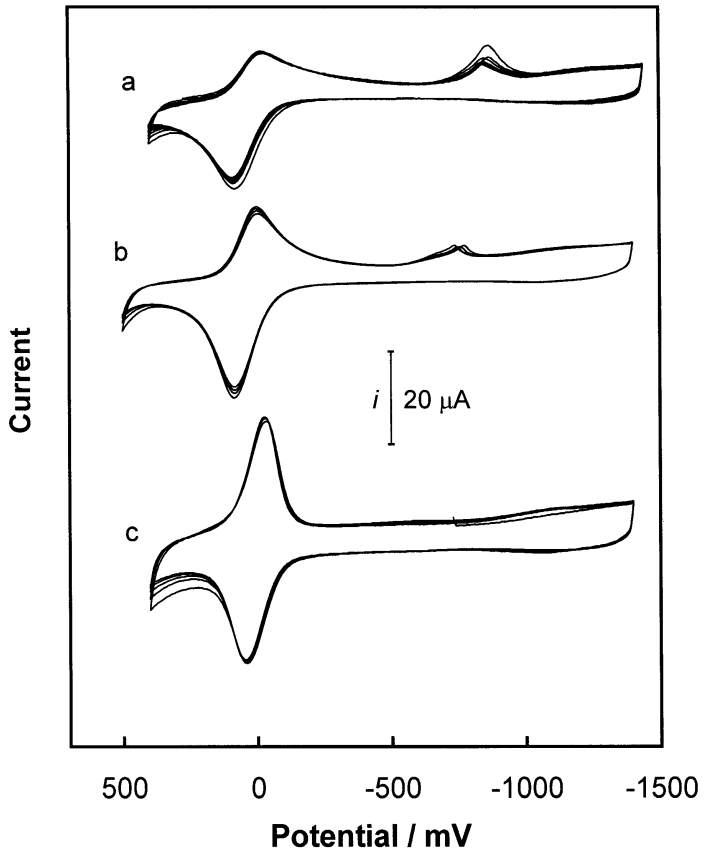

Figure 6. Cyclic voltammograms for the FcC_{60}/Pt films in acetonitrile containing 0.10 M tetra(*n*-butyl) ammonium perchlorate with no electroactive solute. The sweep rate was 100 mV/s. The FcC_{60}/Pt films were grown under cyclic voltammetry conditions in an acetonitrile-toluene (1:4, *v:v*) containing 0.10 M tetra(*n*-butyl)ammonium perchlorate, 0.40 mM FcC_{60} and (a) 0.27 mM $[Pt(\mu\text{-}Cl)Cl(C_2H_4)]_2$, (b) 0.68 mM $[Pt(\mu\text{-}Cl)Cl(C_2H_4)]_2$, and (c) 1.36 mM $[Pt(\mu\text{-}Cl)Cl(C_2H_4)]_2$.

FcC_{60} are shown in Fig. 7. In contrast to the behavior observed for the film formed in solution with a low platinum complex concentration, the cathodic and anodic peak currents depend linearly on the sweep rate for the entire potential sweep rate range 10 to 500 mV/s. However, the difference between the anodic and cathodic peak potentials still depends on the sweep rate. The ΔE_p values are much lower (Fig. 7) than those obtained for the film formed in solution of lower concentration of the platinum complex as seen in Fig. 6. The difference between the anodic and cathodic peak potentials is 16 mV for a sweep rate of 10 mV/s. It is also intriguing that the width of the anodic O_1 peak (half-height, 152 mV) is larger than the width of the cathodic peak R_1 (half-height, 105 mV). The specific resistance of the film, calculated on the base of

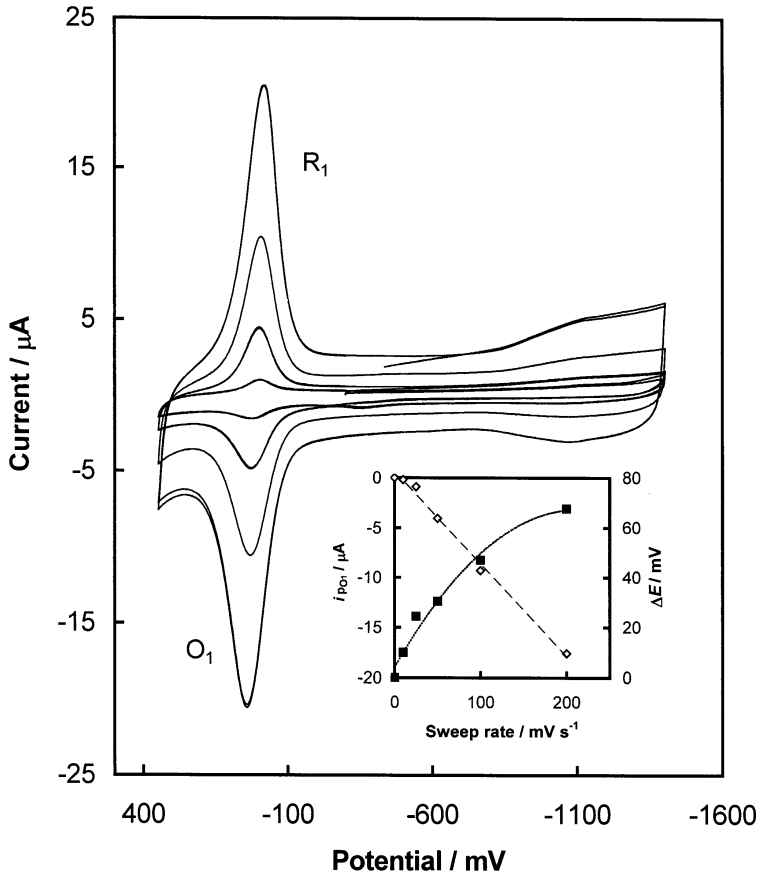

Figure 7. Cyclic voltammograms for the FcC_{60}/Pt film in acetonitrile containing 0.10 M tetra(*n*-butyl) ammonium perchlorate with no electroactive solute for different sweep rates: 25 (innermost), 50, 100 and 200 mV/s (outermost). The dependence of the O_1 peak current (open diamonds) and the difference between the anodic, O_1, and cathodic, R_1, peak potentials (solid squares) on the sweep rate are shown in the inset. The FcC_{60}/Pt film was grown under cyclic voltammetry conditions in an acetonitrile-toluene (1:4, *v:v*) solution containing 0.29 mM FcC_{60}, 1.72 mM $[Pt(\mu\text{-}Cl)Cl(C_2H_4)]_2$ and 0.10 M tetra(*n*-butyl)ammonium perchlorate as supporting electrolyte.

peak potential shift with sweep rate, is equal to about 1500 Ω m. This value is three times lower than those obtained for the film formed in solution of lower concentration of the platinum complex.

The FcC_{60}/Pt film is more stable during potential cycling than the previously studied FcC_{60}/Pd film [25]. The electrode modified with a FcC_{60}/Pt film exhibits stable voltammetric properties over the potential range –100 to –2100 mV. Moreover, the FcC_{60}/Pt film is relatively stable at positive potentials. In the case of the FcC_{60}/Pd film, structural changes occurred in the polymer during its oxidation at positive potentials. These changes resulted in a significant decrease of the potential range of stable voltammmetric response of the film. The voltammetric behavior of the FcC_{60}/Pt film is much less sensitive to film oxidation.

Decamethylferrocene was used as a redox probe dissolved in solution for the investigation of the structural and conductivity properties of FcC_{60}/Pt film. This reversible probe was chosen because its formal redox potential is less negative than that of fullerene reduction and more negative than the potential of the ferrocene oxidation. The conductivity of the FcC_{60}/Pt film depends on its redox state. Completely oxidized or reduced films are not conductive. However, the conductivity of the redox polymer increases when the film is partially reduced or oxidized [33–35]. Therefore, the redox state of the polymer may affect the voltammetric response of redox couples at the polymer-solution interface.

Fig. 8. shows voltammetric studies of the oxidation of decamethylferrocene at an electrode coated with the FcC_{60}/Pt film. For comparison, the reversible voltammetric response of decamethylferrocene at bare gold electrode is shown in Fig. 8, curve a. The process of decamethylferrocene oxidation depends on the potential range used for film formation and the ratio of precursors concentrations used to prepare the films. Results presented in traces b, c, and d were obtained for the FcC_{60}/Pt film formed in a solution containing a relatively low concentration of platinum complex. Trace b shows voltammograms over the potential range from +350 to –1600 mV. In the first negative-going sweep, there is no peak in the range of the formal potential for the decamethylferrocene$^{o/+}$ reduction. The peak for decamethylferrocene oxidation (O**) is observed at the foot of the anodic peak, O_1, for the film oxidation. In the following negative-going sweep, the reduction of the decamethylferrocenium cation (R*) occurs at potentials close to the formal potential of the decamethylferrocene$^{o/+}$ system (curve a in Fig. 8). In the second and subsequent cycles, both oxidation and reduction processes occur in the potential range associated with decamethylferrocene oxidation at bare gold electrode. However, the electron exchange in the decamethylferrocene$^{o/+}$ system on the modified electrode is much less reversible than that on the bare gold electrode.

Voltammograms presented in trace c of Fig. 8 were recorded in the potential range 0 to –1400 mV. In this case, small R* and O* peaks are observed along with the O** peak at a potential near the foot of the peak for film oxidation. If the switching potential in the positive-going scan is more negative than the potential for the film oxidation, peaks R* and O* are not observed in the voltammograms (curve d of

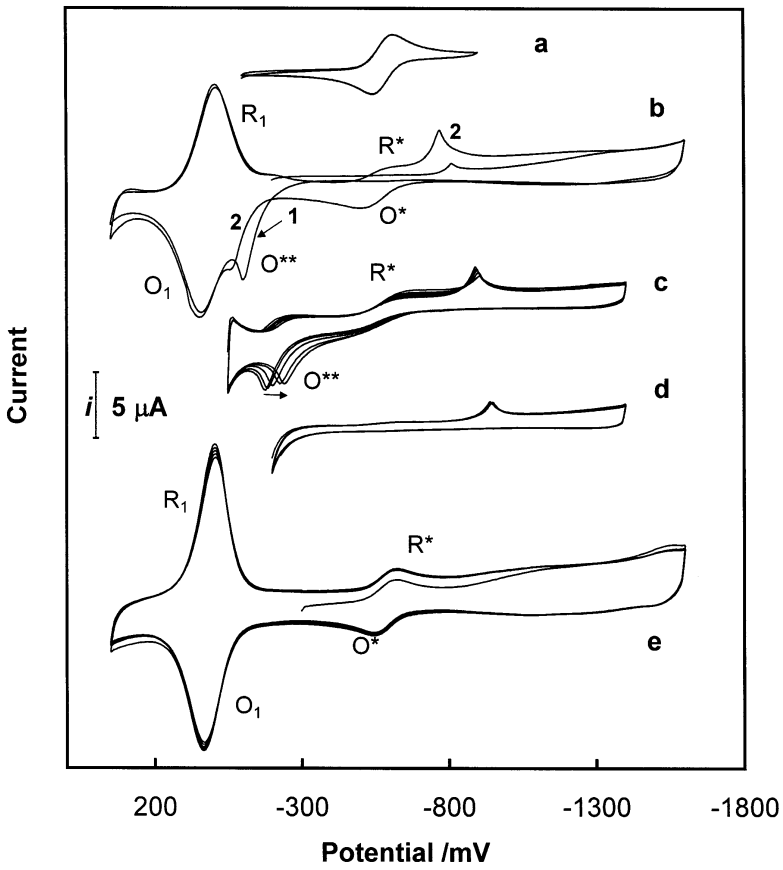

Figure 8. Cyclic voltammograms in acetonitrile containing 1.0 mM decamethylferrocene and 0.10 M tetra(*n*-butyl)ammonium perchlorate at (a) a bare gold disk electrode, (b–d) an electrode coated with the FcC_{60}/Pt film (grown under cyclic voltammetry conditions in an acetonitrile/toluene (1:4, *v:v*) solution containing 0.29 mM FcC_{60}, 0.40 mM $[Pt(\mu\text{-}Cl)Cl(C_2H_4)]_2$ and 0.10 M tetra(*n*-butyl)ammonium perchlorate over the potential range –100 to –1300 mV), (e) an electrode coated with the FcC_{60}/Pt film (grown under cyclic voltammetry conditions in an acetonitrile-toluene (1:4, *v:v*) solution containing 0.29 mM FcC_{60}, 1.72 mM $[Pt(\mu\text{-}Cl)Cl(C_2H_4)]_2$ and 0.10 M tetra(*n*-butyl)ammonium perchlorate in the potential range –100 to –1300 mV). The sweep rate was 100 mV/s.

Fig. 8d). For films formed in a solution containing a low concentration of the platinum complex, the peaks O* and R* are present in voltammograms starting from the first negative going scan when a broader potential range (+350 to –1300 mV) is used during the film formation.

Fig. 8e shows the decamethylferrocene oxidation at an electrode coated with film formed in the potential range –100 to –1300 mV from a solution containing a high ratio of [Pt] to [FcC_{60}]. In this case, reversible decamethylferrocene electron transfer occurs in the potential range seen for decamethylferrocene oxidation at bare gold

electrode. However, the separation between oxidation and reduction peak potentials is higher at the fullerene-modified electrode than at a bare gold electrode.

In the case of the film formed from a solution containing a large concentration of $[Pt(\mu\text{-}Cl)Cl(C_2H_4)]_2$ (1.72 mM), the decamethylferrocene oxidation and reduction peaks are observed in the potential range of the formal potential of the decamethylferrocene$^{o/+}$ redox system both for the film formed in the potential range –100 to –1300 mV as well as for film formed in the range +350 to –1300 mV.

Formation of the FcC_{60}/Ir film. We also tried to prepare FcC_{60}/Ir and FcC_{60}/Rh films by electrochemical reduction of toluene-acetonitrile solutions containing FcC_{60} and either $Ir(CO)_2Cl$(*p*-toluidine) or $Rh_2(CF_3CO_2)_4$. The electrochemical formation of C_{60}/Ir and C_{60}/Rh films has been reported [21]. The voltammetric results obtained for the FcC_{60}/Ir film formation are shown in Fig. 9. In the negative potential range, the

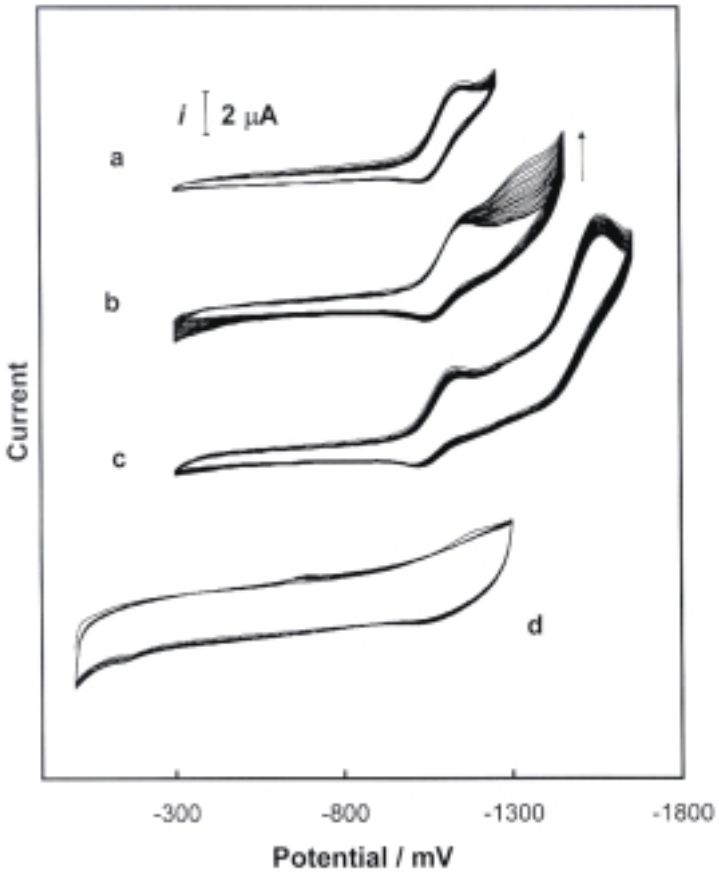

Figure 9. (a–c) Multicyclic voltammograms for 0.25 mM FcC_{60} and 0.55 mM $Ir(CO)_2Cl$(*p*-toluidine) in acetonitrile-toluene (1:4, *v:v*) solution containing 0.10 M tetra(*n*-butyl)ammonium perchlorate over different potential ranges, (d) and multicyclic voltammograms for the electropolymerized FcC_{60}/Ir film transferred to acetonitrile containing 0.10 M tetra(*n*-butyl)ammonium perchlorate. The sweep rate was 100 mV s^{-1}

iridium complex is electrochemically inactive [21]. The FcC_{60}/Ir film is formed on the electrode surface if the potential in the cathodic sweep is more negative than the potential of the second reduction step of FcC_{60}. However, if the switching potential in the cathodic sweep is more negative than –1600 mV, the film is not formed. Presumably, the strong repulsive interactions between negatively charged C_{60} moieties and the structural changes of the film due to counter ion doping are responsible for the instability of the film at negative potentials. Therefore, there is a very narrow potential window for the formation of the FcC_{60}/Ir film. The film transferred to acetonitrile containing only supporting electrolyte shows almost no currents related to fullerene reduction and ferrocene oxidation as seen in trace d of Fig. 9. The deposit cannot be seen on electrode surface with naked eye. However, imaging of the electrode surface by SEM reveals the presence of a new phase in a form of large, irregular grains, *ca*. 3 μm in size (Fig. 10). The film is also very porous.

In the case of a solution containing FcC_{60} and $Rh_2(CF_3CO_2)_4$, no polymer is formed under cyclic voltammetry conditions.

CONCLUSIONS

Polymers of FcC_{60} and transition metal atoms or complexes can be formed by electrochemical reduction of solutions containing FcC_{60} and selected transition metal complexes. The process of film formation depends on the nature of metal or metal complex that, eventually, connects the fullerene moieties. FcC_{60}/Pd and FcC_{60}/Pt

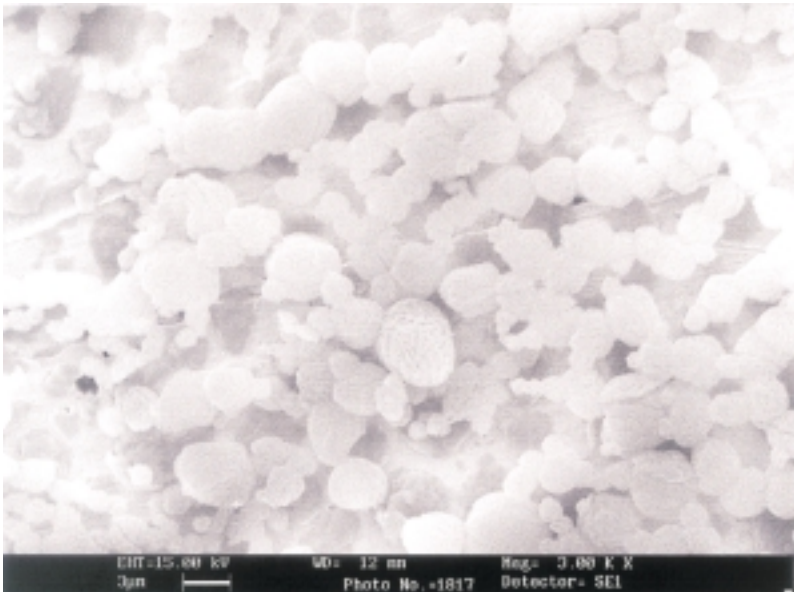

Figure 10. SEM image of the FcC_{60}/Ir film electropolymerized on a gold foil surface under cyclic voltammetry conditions (25 cycles) in the potential range –300 to –1400 mV from 0.25 mM FcC_{60} and 0.55 mM $Ir(CO)_2Cl$(*p*-toluidine) in acetonitrile-toluene (1:4, *v:v*) containing 0.10 M tetra(*n*-butyl)ammonium perchlorate.

films are formed easily with a relatively high yield. However, the process of FcC_{60}/Ir film formation occurs over very narrow potential range, and the yield of the solid polymeric phase formation is very low. It was not possible to produce a film from FcC_{60} and $Rh_2(CF_3CO_2)_4$.

An electroactive film is readily formed by electrochemical reduction of a mixture of FcC_{60} and $[Pt(\mu\text{-}Cl)Cl(C_2H_4)]_2$ in an acetonitrile-toluene (1:4, *v:v*) solution. In this film, the fullerene moieties form part of the polymer backbone and the ferrocene groups are covalently linked to it:

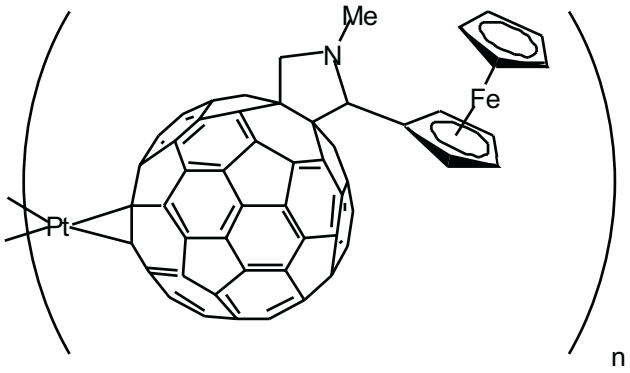

The film is formed in the potential range where both the fullerene and the platinum complex are reduced. Consequently, platinum nanoparticles can be deposited onto the already growing polymeric phase. Results obtained for C_{60}/Pd [26,28,29] and C_{60}/Pt [22] films show that the formation of metallic particles is a key factor that influences the electrochemical properties of the polymer. The deposition of platinum nanoparticles can influence the morphology and redox behavior of FcC_{60}/Pt film as well.

Generally, the electrochemical properties of the FcC_{60}/Pd and FcC_{60}/Pt films are similar. However, some differences can be noticed. First of all, the charge related to the fullerene reduction process at negative potentials is very low for the FcC_{60}/Pt films. The charge is almost independent of the composition of the growth solution and of the supporting electrolyte (Fig. 5 and 6). In the case of FcC_{60}/Pd films, the same behavior was observed only for the film formed in solution containing a large excess of the palladium precursor [25]. It is very likely that the film containing large amount of metallic (platinum or palladium) clusters is responsible for such properties. The structure of these films is not capable of accepting transport of the large tetra(*n*-alkyl) ammonium cations into the polymer layer buried deeply in the film (*i.e.*, located closer to the electrode surface). Therefore, only a surface portion of the film can be reduced.

In the case of the FcC_{60}/Pt film, the negative shift of the reduction potential during the film formation (Fig. 1a) indicates that the reduction processes are inhibited by the film growing on the electrode surface. The potential of film reduction in acetonitrile/toluene (1:4, *v:v*) is more negative than the potentials for reduction of

either C_{60} or the platinum precursor. Partial reduction of the film results in increase of the film's conductivity, and electron exchange on the surface of the film is possible. However, if the film is formed over a larger potential range (*i.e.*, if in the positive-going scan the switching potential is more positive than the potential of peak O_1) an inhibition effect is not observed for reduction processes during the film formation. Probably, the more porous structure of the film formed under these conditions allows penetration of the film by the reactant.

The results of the study of the electrochemical oxidation of decamethylferrocene on the electrode coated with the FcC_{60}/Pt film are very useful in understanding the conductivity mechanism of the film. That is, the conductivity of the FcC_{60}/Pt film depends on conditions of the film formation. The film formed in the potential range from –100 to –1300 mV from a solution containing a low ratio of [Pt] to [FcC_{60}] (lower than about 1) are not conductive over the range between the potential of film oxidation (about 0 mV) and film reduction (about –1000 mV). In the first positive-going scan, the oxidation of decamethylferrocene is not observed at potentials close to the formal potential of the decamethylferrocene$^{o/+}$ redox system. The oxidation of the redox probe occurs in the potential range of FcC_{60}/Pt film oxidation. Partial oxidation of the film results in an increase of its conductivity, and the transport of electrons through the film is possible. The oxidation of the film irreversibly changes its conductivity. The film becomes conductive. In the second and subsequent cycles, the oxidation of decamethylferrocene is observed in the potential range of the formal potential of decamethylferrocene$^{o/+}$ redox system. Similar behavior is observed for the film formed in the potential range from +350 to –1300 mV.

The films formed in solution containing a large ratio of [Pt] to [FcC_{60}] (higher than about 3) are likely to contain microcrystals of metallic platinum. It this system, electrons can be transferred between different polymeric chains through the conductive Pt nanoclusters. Hence, the conductivity of the film increases. The contribution of the metallic phase to the conductivity of the film is high enough to make it conductive even in the potential range from 0 mV to –1000 mV. Similar behavior was observed for the C_{60}/Pd film formed from solutions containing a large excess of palladium(II) acetate [29].

The FcC_{60}/Ir film is formed on the electrode surface during the reduction of FcC_{60} in the presence of $Ir(CO)_2Cl$(*p*-toluidine) in an acetonitrile-toluene (1:4, *v:v*) mixture. By analogy to the C_{60}/Ir film [21], it can be assumed that C_{60} cages are bound through the -$Ir(CO)_2$- spacers. This film has limited prospects for application because it is electrochemically inactive in a solution containing only supporting electrolyte.

Acknowledgments

We thank to the Polish State Committee for Scientific Research (grant 3T09A04626 to K.W.) and the National Science Foundation (grant CHE0070291 to A.L.B.) for financial support. We also gratefully acknowledge Dr. M. Donten from the Department of Chemistry of Warsaw University for rendering us access to the scanning electron microscope.

REFERENCES

1. Diaz A.F., Kanazawa K.K. and Gardini G.P., *J. Chem. Soc., Chem. Commun.*, 635 (1979).
2. Petitjean J., Aeiyach S., Lacroix J.C. and Lacaze, *J. Electroanal. Chem.,* **478**, 92 (1999).
3. Zhou M., Pagels M., Geschke B. and Heinze J., *J. Phys. Chem. B,* **106**, 10065 (2002).
4. Diaz A.F. and Logan J.A., *J. Electroanal. Chem.,* **111**, 111 (1980).
5. Inzelt G., *J. Electroanal. Chem.,* **279**, 169 (1990).
6. Lindfors T. and Ivaska A., *J. Electroanal. Chem.,* **531**, 43 (2002).
7. Rasch, B. and Vielstich W., *J. Electroanal. Chem.*, **370**, 109 (1994).
8. Gofer Y., Killian J.G., Sarker H., Poehler T.O. and Searson P.C., *J. Electroanal. Chem.,* **443**, 103 (1998).
9. Huchet L., Akoudad S., Levillain E., Roncali J., Emge A. and Bauerle P., *J. Phys. Chem. B,* **102**, 7776 (1998).
10. Inzelt G., in Electroanalytical Chemistry, Vol. 18, Ed. Bard A.J., Marcel Dekker, New York, 1994, p. 89.
11. Molecular Design of Electrode Surfaces, Techniques of Chemistry, Vol. 22, Ed. Murray R.W., Wiley, New York, 1992.
12. Electroactive Polymer Electrochemistry, Part 2, Ed. Lyons M.E.G., Plenum Press, New York, 1996.
13. Evans G.P., in: Electrochemical Science Engineering, Vol. 1, Eds. Gerischer H., Tobias C.W., VCH Press, Weinheim, 1999, p. 1.
14. Xie Q., Perez-Cordero E. and Echegoyen L., *J. Am. Chem. Soc.,* **114**, 3978 (1992).
15. Xie Q., Arias F. and Echegoyen L., *J. Am. Chem. Soc.,* **115**, 9818 (1993).
16. Anderson H.L., Boudon C., Diedrich F., Gisselbrecht J.-P., Gross M. and Seiler P., *Angew. Chem., Int. Ed. Engl.,* **33**, 1628 (1994).
17. Benincori T., Brenna E., Sannicolo F., Trimarco L., Zoti G. and Sozzani P., *Angew. Chem., Int. Ed. Engl.,* **35**, 648 (1996).
18. Fedurco M., Costa D., Balch A.L. and Fawcett W.R., *Angew. Chem., Int. Ed. Engl.,* **34**, 194 (1995).
19. Winkler K., Costa D.A., Balch A.L. and Fawcett W.R., *J. Phys. Chem.,* **99**, 17431 (1995).
20. Winkler K., Costa D.A., Fawcett W.R. and Balch A.L., *Adv. Mat.*, **9**, 153 (1997).
21. Balch A.L., Costa D.A. and Winkler K., *J. Am. Chem. Soc.,* **120**, 9614 (1988).
22. Hayashi A., de Bettencourt-Dias A., Winkler K. and Balch A.L., *J. Mater. Chem.,* **12**, 2116 (2002).
23. Cravino A., Zerza G., Neudebauer H., Maggini M., Bucella S., Menna E., Svensson M., Andersson M.R., Brabec C. and Sariciftci N.S., *J. Phys. Chem. B,* **106**, 70 (2002).
24. Cravino A. and Sariciftci N.S., *J. Mater. Chem.,* **12**, 1931 (2002).
25. Plonska M.E., de Bettencourt-Dias A., Balch A.L. and Winkler K., *Chem. Mater.,* **15**, 4122 (2003).
26. Winkler K., de Bettencourt-Dias A. and Balch A.L., *Chem. Mater.*, **11**, 2265 (1999).
27. Winkler K., de Bettencourt-Dias A. and Balch A.L., *Chem. Mater.*, **12**, 1386 (2000).
28. Winkler K., Noworyta K., Kutner W. and Balch A.L., *J. Electrochem. Soc.*, **147**, 2597 (2000).
29. Winkler K., Noworyta K., Sobczak J.W., Wu C.-T., Chen L.-C., Kutner W. and Balch A.L., *J. Mater. Chem.,* **13**, 518 (2003).
30. Prato M., Maggini M., Giacometti C., Scorrano G., Sandona G. and Farnia G., *Tetrahedron*, **52**, 5221 (1996).
31. Prato M., Maggini M. and Scorrano G., *Synth. Met*., **77**, 89 (1996).
32. Klabunde U., *Inorg. Synth*., **15**, 82 (1974).
33. Ofer D., Crooks R.M. and Wrighton M.S., *J. Am. Chem. Soc.,* **112**, 7869 (1990).
34. Paul E.W., Ricco A.J. and Wrighton. M.S., *J. Phys. Chem.,* **89**, 1441 (1985).
35. Thackeray J.W., White H.S. and Wrighton M.S., *J. Phys. Chem.,* **89**, 5133 (1985).